

67-FM-87



NATIONAL AERONAUTICS AND SPACE ADMINISTRATION

## MSC INTERNAL NOTE NO. 67-FM-87

June 30, 1967

# USE OF PLANETARY OBLATENESS FOR PARKING ORBIT OPERATIONS FOR INTERPLANETARY MISSIONS

By Joseph R. Thibodeau III

Advanced Mission Design Branch



TECHNICAL LIBRARY  
BELLCOIN, INC.  
955 L'Enfant Plaza North, S.W.  
Washington, D. C. 20024



MISSION PLANNING AND ANALYSIS DIVISION  
MANNED SPACECRAFT CENTER  
HOUSTON, TEXAS

(NASA-TM-X-69687) USE OF PLANETARY  
OBLATENESS FOR PARKING ORBIT OPERATIONS  
FOR INTERPLANETARY MISSIONS (NASA) 28 p

N74-70493

Unclas  
00/99 16128

MSC INTERNAL NOTE NO. 67-FM-87

---

USE OF PLANETARY OBLATENESS FOR PARKING ORBIT  
OPERATIONS FOR INTERPLANETARY MISSIONS

By Joseph R. Thibodeau III  
Advanced Mission Design Branch

---

June 30, 1967

MISSION PLANNING AND ANALYSIS DIVISION  
NATIONAL AERONAUTICS AND SPACE ADMINISTRATION  
MANNED SPACECRAFT CENTER  
HOUSTON, TEXAS

Approved:   
Jack Funk, Chief  
Advanced Mission Design Branch

Approved:   
John P. Mayer, Chief  
Mission Planning and Analysis Division

## CONTENTS

Section	Page
SUMMARY . . . . .	1
INTRODUCTION . . . . .	1
SYMBOLS . . . . .	2
TECHNIQUE FOR ORBITAL OPERATIONS . . . . .	3
DERIVATION . . . . .	5
Determination of Orbital Inclination . . . . .	6
Determination of Orbital Eccentricity . . . . .	11
A Fortran Computer Program Using This Technique . . . . .	14
Coordinate systems . . . . .	14
A PRELIMINARY ANALYSIS OF A 1975 MARS ORBITAL MISSION . . . . .	15
Procedure . . . . .	15
Results . . . . .	15
EVALUATION OF FUEL COSTS FOR ORBITAL ALIGNMENT . . . . .	17
REFERENCES . . . . .	23

## FIGURES

Figure		Page
1	Geometry of the parking orbit at the time of arrival and departure . . . . .	4
2	Geometry of trajectory planes (Taken from Ref- erence 3) . . . . .	7
3	Velocity to brake into and inject from a re- gressing parking orbit . . . . .	20
4	Determining the characteristics of feasible parking orbits . . . . .	21
5	Variation of Mars parking orbit inclination and eccentricity with stay time . . . . .	22

# USE OF PLANETARY OBLATENESS FOR PARKING ORBIT OPERATIONS FOR INTERPLANETARY MISSIONS

By Joseph R. Thibodeau III

## SUMMARY

A technique for parking orbit operations has been developed to aid stay time analysis of the orbital phases of a planetary reconnaissance or landing mission. This technique takes advantage of a planet's gravitational perturbations to rotate the parking orbit, thereby eliminating the need for maneuvers to change the orbit plane, line of apsides, or orbital eccentricity. A FORTRAN computer program employing this technique was used to find parking orbits which require no maneuvers for orbital realignment. A preliminary parking orbit and stay time analysis is presented for a 1975 Mars orbital mission to illustrate the feasibility of this technique.

## INTRODUCTION

During planetary reconnaissance or landing missions, parking orbits satisfying mission objectives must be established about the destination planet. Often, these stopover missions require large orbital plane changes and line of apsides rotations while the spacecraft is in the parking orbit. Rotation of the parking orbit becomes necessary because of two dynamical phenomena - the orientation and motion of the hyperbolic departure asymptote and the motion of the parking orbit due to the asphericity of the planet's gravitational field.

Sophisticated operational techniques have been developed to reorient the parking orbit. Several of these techniques are investigated in reference 1. Each of these techniques requires the spacecraft to accurately execute several consecutive maneuvers to reorient the parking orbit. Thus orbital missions are complex, and heavy demands are placed on the spacecraft guidance, navigation, and control systems. It would be highly advantageous to eliminate the need for these maneuvers.

It may be possible to design orbital missions which require no parking orbit maneuvers. For these missions, the mechanism for parking orbit rotation would be the orbital perturbations due to the asphericity of the planet's gravitational field.

This paper develops a technique in which these perturbations continually rotate the orbital plane and line of apsides while the spacecraft is in the parking orbit about the planet. The goal of this technique is to consider only those operations inside the planet's sphere of influence and to freely choose the characteristics of the parking orbit and entry and exit hyperbolas so that they match the interplanetary trajectory at the planet's sphere of influence and require no parking orbit maneuvers except the orbital deboost and injection burns.

# SYMBOLS

$a$	semimajor axis
$e$	orbital eccentricity
$i$	orbital inclination with respect to the planet's equatorial plane
$J_2$	second zonal harmonic of destination planet
$n$	mean motion of the parking orbit
$R$	equatorial radius of destination planet
$r_p$	radius of periapsis
$V_\infty$	excess hyperbolic velocity of the interplanetary trajectory
$\alpha$	planetocentric right ascension
$\delta$	planetocentric declination
$\Delta T$	stay time in parking orbit about destination planet
$\theta$	angle between periapsis and excess hyperbolic velocity vector
$\mu$	gravitational parameter of destination planet
$\sigma$	auxiliary variable = $\sin^{-1} (\tan \delta / \tan i)$

$\hat{\Omega}$	unit vector in the direction of the ascending node
$\dot{\Omega}_s$	nodal regression rate due to planetary oblateness
$\dot{\Omega}_r$	normalized rotation rate
$\omega_p$	argument of periapsis
$\dot{\omega}_s$	periapsis precession rate due to planetary oblateness

#### Subscripts

A	approach trajectory
D	departure trajectory
P	periapsis
$\Omega$	ascending node
$\omega$	argument of periapsis

### TECHNIQUE FOR ORBITAL OPERATIONS

The sequence of maneuvers for this technique is illustrated in figure 1 and outlined as follows:

1. The spacecraft deboosts into parking orbit at periapsis of the arrival hyperbola.

- a. The parking orbit and the arrival hyperbola are coplanar.
- b. The periapsis position vectors of the parking orbit and arrival hyperbola are identical.

2. The spacecraft waits in the parking orbit until the time of departure. During this time, the orbital plane and line of apsides will be in motion due to asphericity of the planet's gravitational field. Also, the position of hyperbolic departure asymptote will vary with time in inertial space due to planetary dynamics.

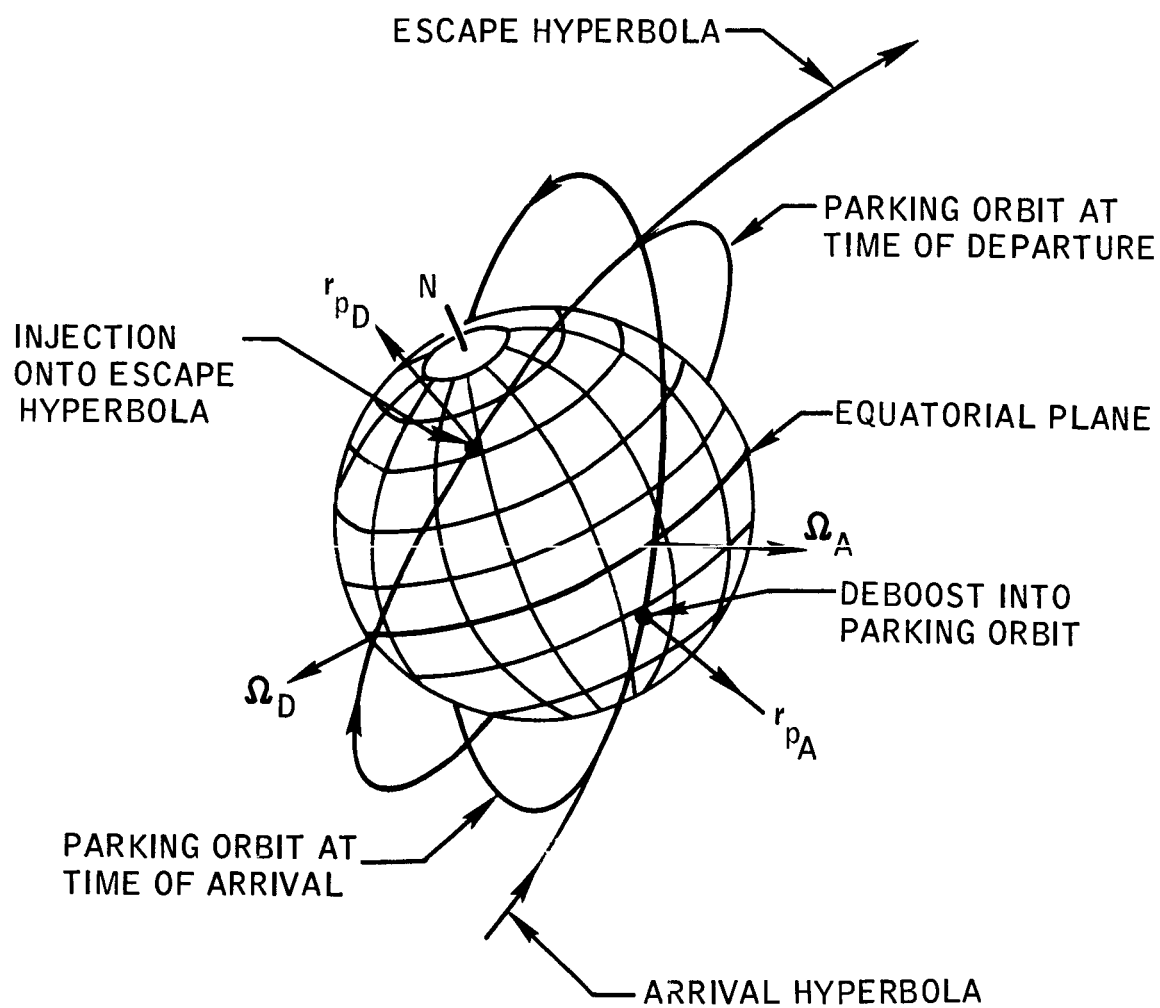


Figure 1. - Geometry of the parking orbit at the time of arrival and departure.



3. At departure, injection onto an escape hyperbola occurs at periapsis of the elliptical parking orbit.

- a. The parking orbit and the escape hyperbola are coplanar.
- b. The periapsis position vectors of the parking orbit and escape hyperbola are identical.

From this outline it is evident that to determine the parking orbit, both the approach and departure trajectories as well as the parking orbit must be considered. The problem is one of determining the orientation of the approach and departure hyperbolas so they match the interplanetary trajectory at the planet's sphere of influence. Likewise, the orientation of the parking orbit must be chosen so that it initially matches the arrival hyperbola, yet will regress during the planetary stay time to match the escape hyperbola.

The boundary conditions for the maneuver sequence are defined by four quantities which are the necessary problem input data:

1. periapsis altitude
2. planetary stay time
3. the  $V_{\infty}$  vector of the interplanetary approach trajectory
4. the  $V_{\infty}$  vector of the interplanetary departure trajectory.

These data are calculated by an independent interplanetary trajectory program (ref. 2). The interplanetary trajectory is assumed to be known, and only those operations inside the planet's sphere of influence are considered.

#### DERIVATION

Given periapsis altitude, the following parameters define the parking orbit size, shape, and orientation:

1. inclination
2. eccentricity
3. longitude of the ascending node
4. argument of periapsis.

This derivation shows how these parameters are found for regressing parking orbits which require no maneuvers except the orbital deboost and injection burns. The orbital parameters are referenced to the time of periapsis passage of the arrival hyperbola.

The determination of the orbital parameters involves two distinct phases. The first phase is a search for the orbital inclination, ascending node, and periapsis vector. The orbital inclination is found by making it the independent search variable. By sweeping through the range of possible inclinations, the node and periapsis vectors and the orbital regression rates can be calculated for each inclination. The proper orbital parameters then are found by interpolation. The second phase finds the orbital eccentricity. The eccentricity is found by using the Newton-Raphson method.

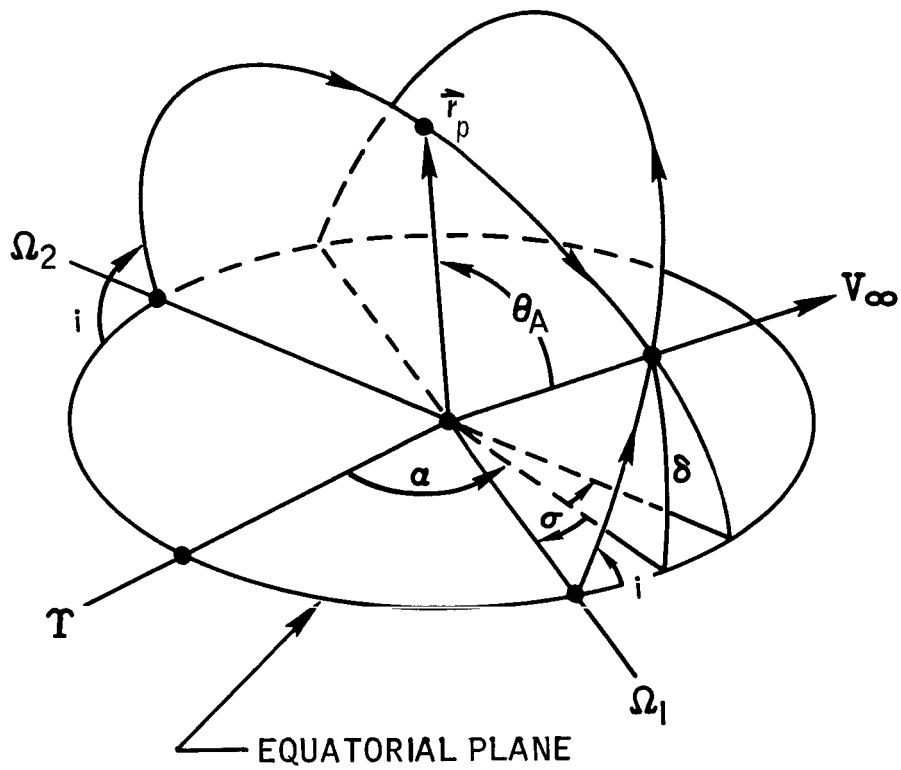
#### Determination of Orbital Inclination

The  $V_{\infty}$  vectors and the periapsis altitude define the characteristics of the approach and departure hyperbolas. They also define limits on the inclination of the approach and departure trajectories as well as the parking orbit. They do not define the plane of the trajectories, however. Two additional vectors are needed to determine the plane of the entry hyperbola and the orientation of the hyperbola within the plane. These vectors are the unit vectors in the direction of the ascending node and periapsis. Since orbital orientation maneuvers are avoided, these vectors are the same for the parking orbit and the arrival hyperbola at the time of periapsis passage on the arrival hyperbola. They can be calculated once the orbital inclination is found.

The node and periapsis position vectors are double-valued functions of inclination. This can be seen in figure 2 which shows there are two orbital planes containing the  $V_{\infty}$  vector for every inclination. Thus, for each inclination, two nodes and two periapsis vectors must be found for each  $V_{\infty}$  vector.

The longitude of the ascending node ( $\alpha_{\Omega}$ ) is determined from the formula:

$$\left. \begin{aligned} \alpha_{\Omega_1} &= \alpha - \sigma \\ \alpha_{\Omega_2} &= \alpha + \sigma + \pi \end{aligned} \right\} \quad (1)$$



NOTE: THERE ARE TWO ORBITS CONTAINING THE TARGET VECTOR FOR EVERY INCLINATION.

Figure 2. - Geometry of trajectory planes.  
(Taken from Reference 3)

where

$$\sigma = \sin^{-1} \left( \frac{\tan \delta}{\tan i} \right)$$

and  $\alpha$  and  $\delta$  are the right ascension and declination of the  $V_{\infty}$  vector.  $\alpha_{\Omega_1}$  is the longitude of the ascending node closest to the  $V_{\infty}$  vector as shown in figure 2. Likewise,  $\alpha_{\Omega_2}$  is the longitude of the node furthest from the  $V_{\infty}$  vector.

The semimajor axis ( $a$ ) of the approach hyperbola is determined from the vis viva equation

$$a = \frac{\mu}{V_{\infty A}^2} \quad (2)$$

When the periapsis radius is specified, the eccentricity of the entry hyperbola can be found by

$$e = \frac{r_p}{a} + 1 \quad (3)$$

The angle between the arrival  $V_{\infty}$  vector and the periapsis of the arrival hyperbola ( $\theta$ ) can now be found by

$$\theta = \cos^{-1} \left( \frac{1}{e} \right) \quad (4)$$

where  $e$  is the eccentricity of the arrival hyperbola.

The argument of periapsis ( $\omega_p$ ) for the arrival hyperbola is found from the following equation

$$\omega_p = \cos^{-1}(\hat{\Omega} \cdot \hat{V}_{\infty}) - \theta \quad (5)$$

At the time of periapsis passage, the argument of periapsis of the parking orbit is the same as for the arrival hyperbola.

The same equations are used to find the node and periapsis vectors

at the time of injection onto the escape hyperbola with one exception:

$$\theta = \cos^{-1} \left( \frac{-1}{e} \right) \quad (6)$$

where  $e$  is the eccentricity of the departure hyperbola.

Suppose the right ascension of the ascending node,  $\alpha_\Omega$ , and the argument of periapsis,  $\omega_p$ , have been calculated for the node closest to the  $V_\infty$  vector for both the arrival and departure hyperbolas. Again considering figure 1, during the planet stay time  $\Omega_A$  must move to  $\Omega_D$ , and  $r_{pA}$  must move to  $r_{pD}$ .

The angular distance the node must travel is

$$\Delta\alpha_\Omega = \alpha_{\Omega_D} - \alpha_{\Omega_A} = f(V_{\infty_A}, V_{\infty_D}, r_p, i) \quad (7)$$

where the subscripts A and D indicate the arrival and departure hyperbolas, respectively.

Likewise, the angular distance the periapsis vector ( $r_p$ ) must travel is

$$\Delta\omega_p = \omega_{pD} - \omega_{pA} = g(V_{\infty_A}, V_{\infty_D}, r_p, i) \quad (8)$$

The speed of rotation of the node ( $\dot{\Omega}_s$ ) and periapsis ( $\dot{\omega}_s$ ) due to secular variation ( $J_2$ ) is given in reference 4 as

$$\dot{\Omega}_s = \frac{-3nJ_2R^2}{2a^2(1-e^2)^2} \cos i \quad (9)$$

$$\dot{\omega}_s = \frac{-3nJ_2R^2}{2a^2(1-e^2)^2} \left( \frac{5}{2} \sin^2 i - 2 \right) \quad (10)$$

Since the fastest rates are experienced by circular orbits, these equations are solved by setting  $e = 0$ .

The time for the node of a circular orbit to traverse  $\Delta\alpha_\Omega$  is

$$\Delta T_\Omega = \left. \frac{\Delta\alpha_\Omega}{\dot{\Omega}_s} \right|_{e=0} \quad (11)$$

and the time for the periapsis to traverse  $\Delta\omega_p$  is

$$\Delta T_\omega = \left. \frac{\Delta\omega_p}{\dot{\omega}_s} \right|_{e=0} \quad (12)$$

If the stay time in the parking orbit is designated by  $\Delta T$ , the problem is to obtain the inclination and eccentricity of the parking orbit such that

$$\Delta T = \Delta T_\Omega = \Delta T_\omega \quad (13)$$

This condition is obtained in two steps.

1. Find a parking orbit inclination that will make  $\Delta T_\Omega$  equal to  $\Delta T_\omega$ .
2. Adjust the parking orbit eccentricity to make  $\Delta T_\Omega$  and  $\Delta T_\omega$  equal to the planet stay time,  $\Delta T$ .

A simple interpolation scheme lends itself to finding the orbital inclination for which  $\Delta T_\Omega$  equals  $\Delta T_\omega$ . If  $\Delta T_\Omega$  and  $\Delta T_\omega$  are calculated at  $10^\circ$  increments through the interval of possible inclinations, the ratio  $\Delta T_\Omega/\Delta T_\omega$  can be tabulated with inclination. Equality of  $\Delta T_\Omega$  and  $\Delta T_\omega$  is indicated by a ratio of unity. Thus the table can be scanned to find a ratio near 1, and the inclination can be found by interpolation.

The interpolated value of inclination can now be used to calculate the  $\Delta T_\Omega$  and  $\Delta T_\omega$  for a circular orbit. If necessary, the above procedure can be repeated using a smaller inclination increment to make  $\Delta T_\Omega$  and  $\Delta T_\omega$  equal within some specified tolerance.

### Determination of Orbital Eccentricity

The orbital eccentricity must now be adjusted so that the orbit will rotate the required amount during the planetary stay time,  $\Delta T$ . The circular orbit rotates through the required angles during the time

$$\Delta T' = \Delta T_{\Omega} = \Delta T_{\omega}$$

A simple test for the existence of an elliptical orbit that regresses the proper amount during the stay time  $\Delta T$  is

$$\Delta T' \leq \Delta T$$

Since circular orbits have the fastest regression rates, this inequality means that the eccentricity can be increased to slow down the speed of rotation and thereby force  $\Delta T'$  to equal  $\Delta T$ .

The eccentricity that makes  $\Delta T'$  equal to  $\Delta T$  can be found quite readily by the Newton-Raphson technique. The orbital eccentricity is a real root of a fourth order polynomial found by expressing equation (9) or (10) in terms of the eccentricity. The derivation of this polynomial and the solution for orbital eccentricity is as follows.

The rate of secular variation of the node and periapsis vectors is given by:

$$\dot{\Omega}_s = \frac{-3nJ_2 R^2}{2a^2(1 - e^2)^2} \cos i \quad (9)$$

$$\dot{\omega}_s = \frac{-3nJ_2 R^2}{2a^2(1 - e^2)^2} \left( \frac{5}{2} \sin^2 i - 2 \right) \quad (10)$$

Note that the rate ratio,  $\frac{\dot{\Omega}_s}{\dot{\omega}_s}$ , is determined by the inclination since the terms involving eccentricity divide out in the ratio. Thus the eccentricity can be adjusted independently to change the rate without destroying a particular value of the ratio.

Designate the common factor in both equations by  $\dot{\Omega}_r$ . Then

$$\dot{\Omega}_r = \frac{-3nJ_2 R^2}{2a^2(1 - e^2)^2} \quad (14)$$

and equations (9) and (10) become

$$\dot{\Omega}_s = \dot{\Omega}_r \cos i \quad (15)$$

$$\dot{\omega}_s = \dot{\Omega}_r \left( \frac{5}{2} \sin^2 i - 2 \right) \quad (16)$$

The mean motion (n) is given by

$$n = \sqrt{\frac{\mu}{a^3}} \quad (17)$$

The semimajor axis (a) is

$$a = \frac{r_p}{1 - e} \quad (18)$$

By substituting for n and a into equation (14) and simplifying, the following result is obtained:

$$\dot{\Omega}_r = \left\{ -\frac{3}{2} \sqrt{\mu} J_2 R^2 r_p^{-7/2} \right\} (1 - e)^{3/2} (1 + e)^{-2} \quad (19)$$

For a given periapsis radius, the quantity in curly brackets is constant. Let

$$C = \left\{ -\frac{3}{2} \sqrt{\mu} J_2 R^2 r_p^{-7/2} \right\} \quad (20)$$

Then

$$K = (1 - e)^{3/2} (1 + e)^{-2} \quad (21)$$

where

$$K = \frac{\dot{\Omega}_r}{C} \quad (22)$$

The problem now is, given K, find e. Squaring both sides of (21) and simplifying the result is

$$K^2 (1 + e)^4 = (1 - e)^3 \quad (23)$$



Expanding (23) in a binomial expansion and collecting common powers of  $e$ , the following result is obtained:

$$e^4 + \frac{(4K^2 + 1)}{K^2} e^3 + \frac{(6K^2 - 3)}{K^2} e^2 + \frac{(4K^2 + 3)}{K^2} e + \frac{K^2 - 1}{K^2} = 0 \quad (24)$$

Equation (24) will have a real root on the interval

$$0 \leq e < 1$$

provided

$$\Delta T' \leq \Delta T$$

Equation (24) is of the form

$$f(x) = x^4 + a_1 x^3 + a_2 x^2 + a_3 x + a_4 = 0 \quad (25)$$

The derivative with respect to  $x$  is

$$f'(x) = 4x^3 + 3a_1 x^2 + 2a_2 x + a_3 = 0 \quad (26)$$

The constant coefficients are

$$\left. \begin{aligned} a_1 &= \frac{4K^2 + 1}{K^2} & a_2 &= \frac{6K^2 - 3}{K^2} \\ a_3 &= \frac{4K^2 + 3}{K^2} & a_4 &= \frac{K^2 - 1}{K^2} \end{aligned} \right\} \quad (27)$$

The constant  $K$  is easily evaluated

$$K = \frac{\dot{\Omega}_r}{C} = \frac{\dot{\Omega}_s}{C \cos i} = \frac{\Delta \alpha_{\Omega} / \Delta T}{C \cos i} \quad (28)$$

where  $C$  is evaluated in equation (2).

The parking orbit eccentricity is found by iteration using equations (25) and (26) in the following formula:

$$e_{n+1} = e_n - \frac{f(e_n)}{f'(e_n)} \quad (29)$$

Since  $e$  is between 0 and 1, the formula quickly converges when an initial estimate of  $e = 0.5$  is used.

#### A Fortran Computer Program Using this Technique

The technique discussed has been programmed. The program is essentially a search routine. It accepts two  $V_\infty$  vectors, one for the approach trajectory and one for the departure trajectory. The  $V_\infty$  vectors define a range of permissible values of inclination for the approach and departure trajectories. Any parking orbit whose inclination falls within this range could conceivably be used if enough fuel is available to make the required plane changes.

The program scans through all the possible inclinations and then uses the above discussed interpolation scheme and a Newton-Raphson technique to determine the characteristics of those parking orbits which match the approach and departure trajectories.

In general, more than one feasible orbit exists. The program outputs all orbits which match the arrival and departure trajectories. The output consists of the Keplerian elements of the parking orbit, the entry hyperbola, and the exit hyperbola.

Coordinate systems.— The input velocity vectors are referenced to a heliocentric ecliptic coordinate system. This is a right-handed rectangular Cartesian system with the positive x-axis pointed toward the vernal equinox, the positive y-axis in the ecliptic plane  $90^\circ$  East of x, and z normal to the ecliptic plane and positive to the North.

The internal coordinate system of the program (and the system to which the output data are referenced) is a planetocentric equatorial system, which is a right-handed rectangular Cartesian system. The x-y plane is defined by the planet's equatorial plane. The positive x-axis points toward the ascending node of the Sun's apparent path around the planet, the positive y-axis is  $90^\circ$  East of x, and the positive z-axis points North along the planet's spin axis. For Earth this is the reference system of celestial coordinates, and the transformation is well known. The transformation to these coordinates for Mars is discussed in detail in reference 5.

## A PRELIMINARY ANALYSIS OF A 1975 MARS ORBITAL MISSION

### Procedure

A preliminary stay time analysis of a 1975 Mars orbital mission has been made. The interplanetary trajectories and the  $V_{\infty}$  vectors at Mars were calculated by an independent trajectory analysis program (ref. 2). The launch date (September 5, 1975) and outbound trip time (303 days) were held constant, and the planet stay times were varied in 50-day increments from 300 to 500 days. The total trip time including the planet stay time varied between 950 and 1170 days so that between one third and one half of the total trip time was spent in parking orbit about the planet.

The  $V_{\infty}$  vectors were used as input data to the parking orbit analysis program. The characteristics of the parking orbit and entry and exit hyperbolas that matched the  $V_{\infty}$  vectors were then determined for each planet stay time. The  $\Delta V$  cost to brake into and inject out of these parking orbits was then calculated.

### Results

The results of this analysis are presented in table I. For each stay time except the 300-day case, there were three possible orbits that satisfied the conditions outlined on page 3.

The  $\Delta V$  cost to deboost into the parking orbit ( $\Delta V_{IN}$ ) and the injection  $\Delta V$  ( $\Delta V_{OUT}$ ) are plotted versus stay time in figure 3. The lower three curves show the cost to deboost into the parking orbit as a function of stay time. Each curve presents the variation in deboost  $\Delta V$  for one particular parking orbit. For a given inclination, these curves will display a downward trend due to variation of the orbital eccentricity with stay time. (The eccentricity variation is discussed below and shown in figure 6.)

The upper three "bucket" shaped curves in figure 3 show the variation in injection  $\Delta V$  as a function of stay time. Each curve presents the variation of injection  $\Delta V$  for one particular parking orbit. The shape of the curve is determined by the variation in magnitude of the departure  $V_{\infty}$  vector.

Two important conclusions regarding a 3-year, 1975 Mars orbital mission can be inferred from table I.

1. The total  $\Delta V$  commitment for parking orbit operations is least for a planetary stay time near 400 days (nearly one third of the total mission time).

2. There exists a parking orbit for which the total  $\Delta V$  commitment for parking orbit operations is less than 6000 fps. In fact, the parking orbit has an inclination of  $145^\circ$  and an eccentricity of 0.76 (table I).

Why did the parking orbit with the  $145^\circ$  inclination have the least  $\Delta V$  requirement and not the one with a  $72^\circ$  or  $100^\circ$  inclination? Part of the answer lies in figure 4, which shows how the parking orbit node and periapsis rotation rates vary with inclination. The figure indicates that (1) near-equatorial orbits experience faster rotational rates than near-polar orbits, and (2) their speed of rotation is less dependent on eccentricity. Thus, if we consider two parking orbits with identical node and periapsis rotation rates - one a near-polar orbit and the other a near-equatorial orbit, the near-equatorial orbit will have the larger eccentricity, and will, therefore, require lower deboost and injection  $\Delta V$ 's. The argument is supported in figure 5(a) which shows that the orbit with the  $145^\circ$  inclination has the highest eccentricity.

Actually, this behavior is not as simple as the argument indicates. Two geometric factors complicate the situation:

1. The declination of the departure asymptote varies with time in inertial space.
2. The angles through which the parking orbit must rotate during the planned stay time vary with inclination.

Both factors affect the characteristics of the parking orbit. The required orbital inclination slowly changes with planned stay time due to variation in declination of the departure  $V_\infty$  vector. Since both inclination and eccentricity mutually affect the orbit rotation rates, the eccentricity also varies to compensate for the change in rate due to inclination. This behavior is illustrated in figure 5(a) and 5(b) where the required orbital inclination and eccentricity are plotted versus planetary stay time.

The situation would be greatly simplified if the departure asymptote did not vary with time. In this case the required orbital inclination would remain fixed over the interval of stay times; and the parking orbit eccentricity would be a simple function of planet stay time. The variation of eccentricity with stay time for this simplified situation is shown in figure 6. The figure was generated based on the  $V_\infty$  geometry for the 400-day stay time. The eccentricity was varied to find out the shortest time required for the orbit to rotate through the required angles ( $\Delta\alpha_\Omega$  and  $\Delta\omega_p$ ). The figure indicates that a circular orbit would rotate through the required angles during a stay time as low as 20 days (for the  $145^\circ$  inclination orbit). However, a plane change would be required for planetary stay times shorter than 20 days.

Figure 6 also explains why the variation in deboost  $\Delta V$  ( $\Delta V_{IN}$ ) shown in figure 3 is so small. The curves are nearly flat on the interval from 300 to 500 days, and the required orbital eccentricity slowly increases with increasing planet stay time; thus the deboost  $\Delta V$  requirement to get into these orbits is slowly decreasing. On the interval from 20 to 100 days, the required orbital eccentricity increases steeply with increasing stay time. Thus for short stay times we would expect the deboost  $\Delta V$  curves of figure 3 to be more steeply down-sloping. Also since near-circular orbits require higher deboost and injection  $\Delta V$ 's than more elliptical orbits, the deboost and injections  $\Delta V$ 's will be displaced upwards in figure 3 for the shorter stay times.

#### EVALUATION OF FUEL COSTS FOR ORBITAL ALIGNMENT

Because this technique requires no maneuvers in orbit does not mean it is free of fuel costs for orbital alignment. The fuel costs for orbit orientation occur at the planet's sphere of influence and parking orbit periapsis.

The  $\Delta V$  required at the planet's sphere of influence, however, is very small compared to other  $\Delta V$  costs. The  $\Delta V$  is required to achieve a given periapsis altitude and inclination of the hyperbolic arrival trajectory. (This penalty is analogous to the cost of pushing a precariously balanced marble off the apex of a right circular cone where the targeting condition is a point at the base of the cone.)

The primary fuel cost is paid at periapsis of the parking orbit. Two major burns occur at this point:

1. The deboost into the parking orbit.
2. The injection onto the escape hyperbola.

The eccentricity of the parking orbit is the fundamental quantity which governs the expense of these maneuvers. The fuel cost for either maneuver is greatest for a circular parking orbit. Assuming periapsis altitude remains fixed, the cost diminishes as orbital eccentricity increases. To save the most fuel, it is therefore advantageous to have the parking orbit eccentricity as large as possible.

Orbital eccentricity also governs the speed of rotation of the orbital node and periapsis position vectors. Circular orbits experience the fastest regression rates. For an orbital mission in which a large plane change must be realized during a short stay time, it may be necessary to adopt a near-circular parking orbit. In that case, less

$\Delta V$  may be required to deboost into a high eccentricity ellipse and make a parking orbit plane change.

The important conclusions regarding use of this technique therefore rest with the tradeoff on orbital eccentricity. Obviously any technique which requires a smaller orbital eccentricity will have greater fuel costs than this technique.

For long planetary stay times (300 to 500 days), this technique appears to be feasible for orbital eccentricities as high as 0.7. Short planetary stay times (20 to 50 days) are being investigated and will be the subject of a future internal note.

TABLE I.- MARS PARKING ORBIT CHARACTERISTICS FOR A  
3-YEAR, 1975 MISSION

Stay time, days	Inclination, deg	Eccentricity, e, nd	$\Delta V_{IN}$ , fps	$\Delta V_{OUT}$ , fps	Periapsis velocity, $V_P$ , fps
300	70.0	0.58	3029	8580	14 249
	112.0	0.53	3256	8876	14 021
350	73.0	0.61	2894	5171	14 383
	111.0	0.56	3119	5396	14 158
	141.0	0.70	2498	4775	14 780
400	72.0	0.62	2850	4280	14 428
	110.5	0.59	2984	4414	14 293
	141.0	0.76	2239	3669	15 038
450	72.0	0.66	2673	5111	14 605
	109.5	0.58	3029	5467	14 249
	141.0	0.78	2154	4592	15 124
500	75.0	0.72	2411	5918	14 867
	110.0	0.60	2939	6446	14 339
	135.0	0.74	2325	5832	14 953

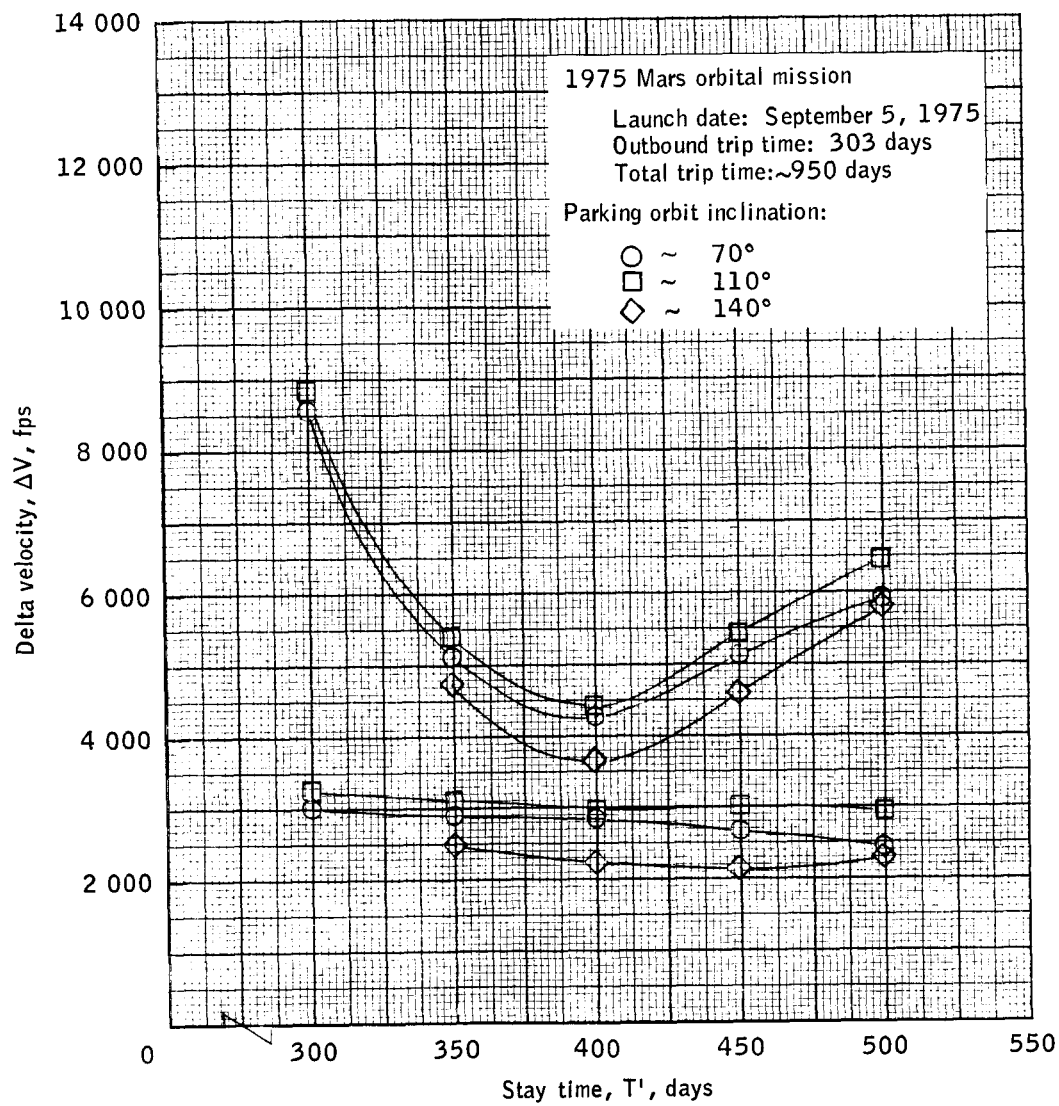


Figure 3.- Velocity to brake into and inject from a regressing parking orbit.



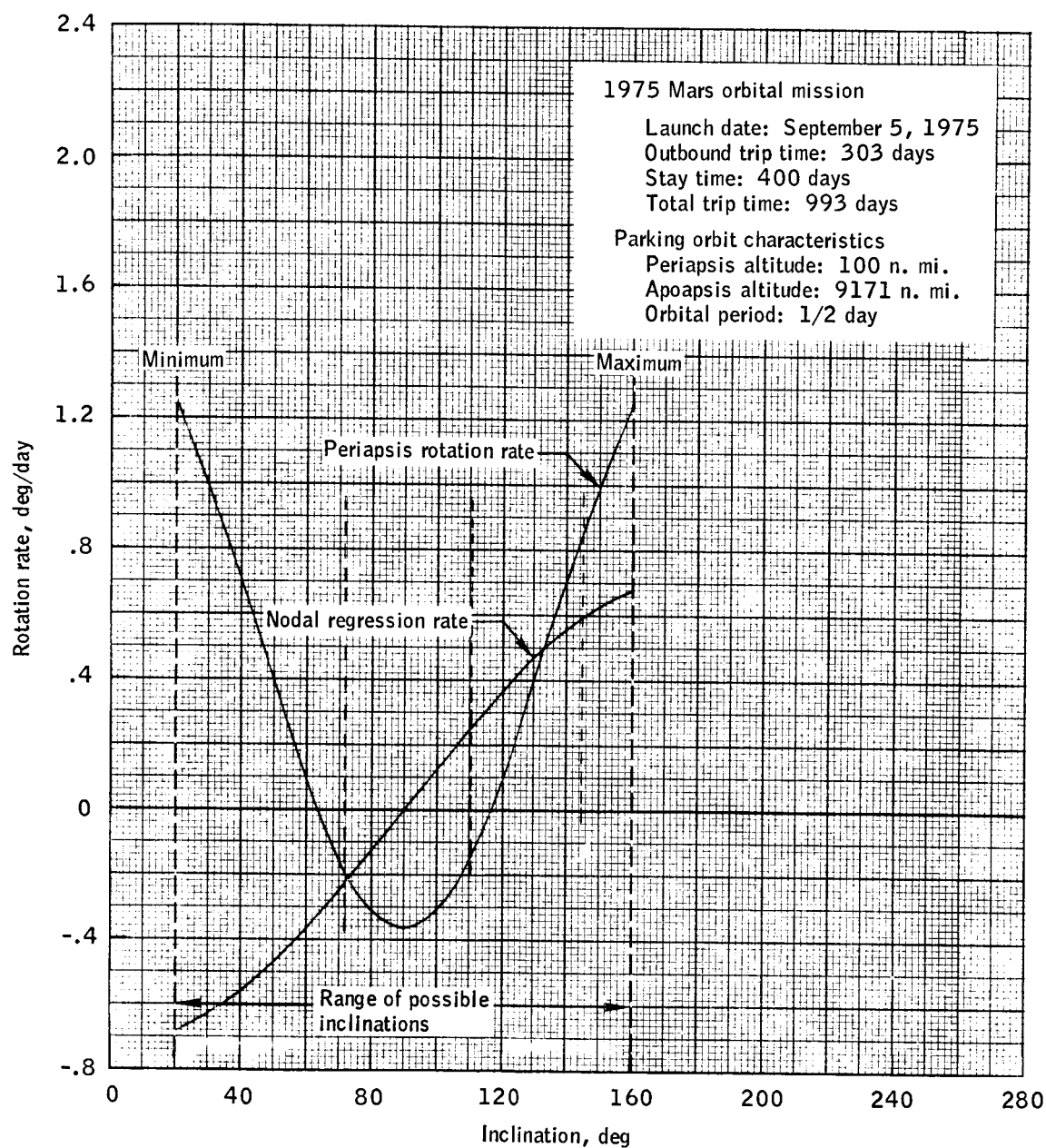


Figure 4.- Determining the characteristics of feasible parking orbits.

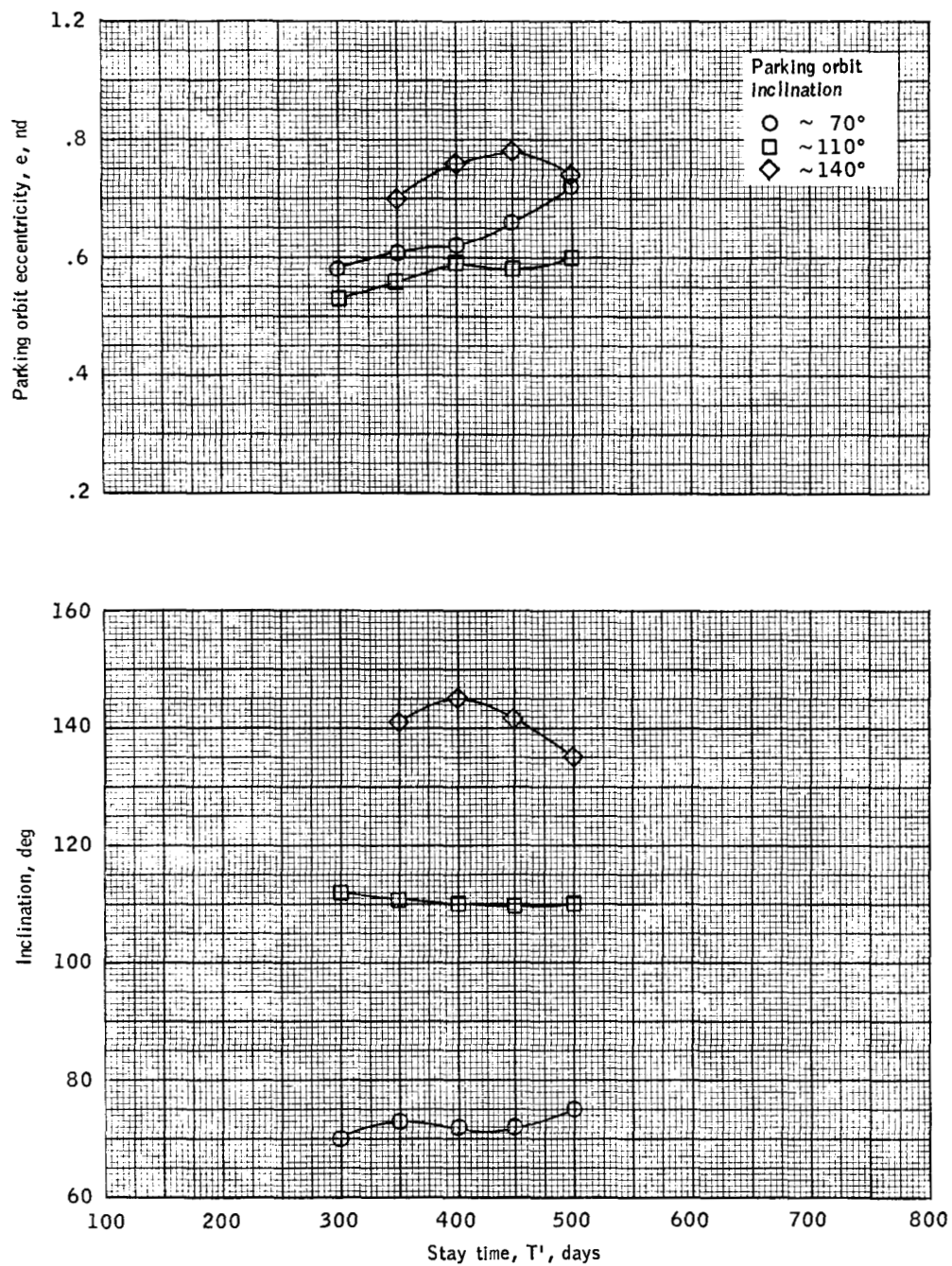


Figure 5.- Variation of Mars parking orbit inclination and eccentricity with stay time.

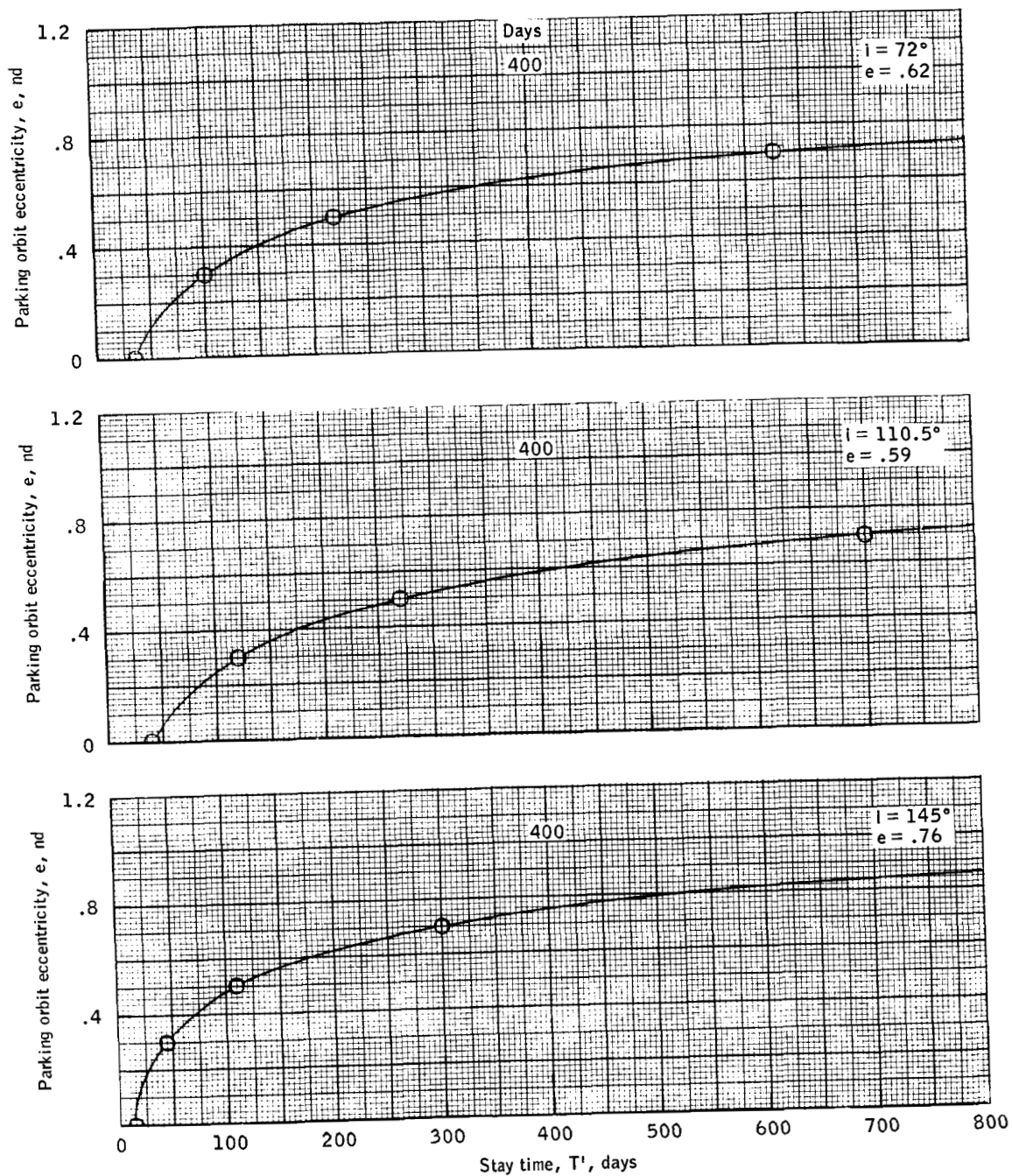


Figure 6.- Required orbital eccentricity as a function of stay time for a stationary departure asymptote.

## REFERENCES

1. Luiden, Roger W.; Miller, Brent A.: Efficient Planetary Parking Orbits with Examples for Mars. NASA TN D-3220, January, 1966.
2. Garland, Benjamine J.: Three-Dimensional Trajectory Analysis of Non-stop Round-Trip Mars Mission Between 1970 and 1988 Using Propulsive-Gravity Turns with Atmospheric Effects. NASA TM X-1122, August, 1965.
3. Battin, Richard H.: Astronautical Guidance. McGraw-Hill Book Co., 1964.
4. Danby, J. M. A.: Fundamentals of Celestial Mechanics. The Macmillan Co., 1962.
5. TRW Systems: Planetocentric Co-ordinate Transformations for the Planet Mars. Summary Technical Report, August 6, 1965.